Conf-9502151--1

LA-UR-94-3871

Title: **A REVIEW OF BROADBAND REGIONAL DISCRIMINATION STUDIES OF NTS EXPLOSIONS AND WESTERN U.S. EARTHQUAKES**

Author(s): **Steven R. Taylor, LANL, Group EES-3, Geophysics**

Submitted to: NATO Advanced Study Institute Conference on CTBT Monitoring
Faro, Algarve, Portugal January 23-February 2, 1995

Los Alamos
NATIONAL LABORATORY

DISCLAIMER

A REVIEW OF BROADBAND REGIONAL DISCRIMINATION STUDIES OF NTS EXPLOSIONS AND WESTERN U.S. EARTHQUAKES

STEVEN R. TAYLOR
Geophysics Group EES-3
Los Alamos National Laboratory
University of California
Los Alamos, NM 87545

Abstract

Verification of a Comprehensive Test Ban Treaty (CTBT) will require the use of regional-distance seismic stations. One important aspect of regional seismic monitoring involves the discrimination of nuclear explosions from other sources such as earthquakes and mining events (e.g. industrial explosions and rockbursts). In this paper, we review earthquake/nuclear explosion discrimination studies in the western U.S. using broad-band seismic data. These studies are important because they are the only ones involving nuclear explosions and other sources in a single geophysical region having excellent ground truth information and a substantial historic database. Additionally, because of access to information from the NTS, much can be learned about the physical basis of regional discriminants. Using multivariate discrimination techniques, it was found that approximately 96% of the events analyzed could be correctly identified down to about magnitude 3.5. Most of the events misidentified were recorded with poor signal-to-noise ratio at only a minimal number of stations. However, a few well-recorded events were misclassified for one or more discriminants. Examples of detailed analysis of a missed violation (nuclear explosion that looks like an earthquake) and a false alarm (naturally occurring event that looks like an explosion) are illustrated. Resolution of anomalous events such as these will be critical to CTBT monitoring.

1. Introduction

On January 25, 1994 the United Nations Conference on Disarmament began negotiations on a multilateral Comprehensive Test Ban Treaty (CTBT). Serious technical problems must be overcome in order to monitor a CTBT to adequate levels on a worldwide basis. The negotiations include monitoring for clandestine nuclear explosions underground, in the oceans, and in the atmosphere. In this paper, we focus our attention on the problem of underground nuclear explosions for which seismic monitoring is the primary observing technology. In addition to detecting and locating events recorded by a seismic network, it is necessary to identify them. This will require discrimination of clandestine nuclear explosions

from other seismic sources such as earthquakes, industrial explosions (e.g. quarry blasts), and other mine seismicity (e.g. rockbursts and collapse events).

For large magnitude events (e.g. m_b > 5) well-established techniques such as the M_S:m_b discriminant can be applied with considerable success (cf. OTA report, 1988). However, for monitoring at lower magnitudes necessary for a CTBT it will be necessary to identify events with m_b < 3 (cf. Hannon, 1985). The CTBT monitoring system should be able to detect and identify nuclear explosions down to a few kilotons or less corresponding to a seismic magnitude of approximately 4 fully tamped or 2.5 fully decoupled. This will require the analysis of regional seismograms and involves numerous technical obstacles. Over the last decade, there have been a plethora of regional discrimination studies in many different geological settings. These studies have found many regional variations in discrimination performance (Baumgart and Young, 1990). Additionally, when characterizing new regions, ground truth information regarding newly recorded events may be unavailable. There may be no historic record of nuclear explosions upon which to base comparisons and the discrimination problem becomes an exercise in outlier detection (c.f. Fisk *et al.*, 1993). Because of data limitations, most discrimination studies have not included all of the different types of sources (nuclear explosions in particular) that will be encountered in monitoring a CTBT.

In this report, we summarize discrimination studies in the western U.S. that have used broadband seismic data. A review of these studies is important because they are the only studies involving nuclear explosions and other sources in a single geophysical region having excellent ground truth information and a substantial historic database. Additionally, because of access to information from the NTS, much can be learned about the physical basis of regional discriminants. We will focus the review on analysis of broadband seismic data from the Livermore NTS Network (LNN) operated by Lawrence Livermore National Laboratory. The first section will review evaluation of discriminants discussed in the summary article of Pomeroy *et al.*, (1982) (Taylor *et al.*, 1989). We then discuss recent work of Walter *et al.*, (1994) involving analysis of high-frequency discriminants. The latter study has additional importance because it analzes two earthquake swarms at different depths located on the NTS which minimizes propagation effects and allows for the examination of depth effects. We finish with a discussion of two misidentified events; a missed violation (misclassified nuclear explosion) and a false alarm (non-nuclear event misclassified as a nuclear explosion). Special event studies of outlier events such as these will be critical in CTBT monitoring.

2. Review of Existing Discriminants at NTS

To explore the issue of regional discrimination, Taylor *et al.*, (1989) analyzed seismic signals from a large number of western U.S. earthquakes and NTS explosions recorded on the LNN. The paper was based on a review of seismic discrimination by Pomeroy *et al.*, (1982) who summarized the use of regional seismic discriminants and concluded that "most have been tested only on limited data, usually from one geographic region and only one or two recording stations. No systematic analyses have been done to determine the best individual discriminant or combination of them." Their major conclusion stated "a systematic

and comparative evaluation of all the proposed regional discriminants is now required, utilizing a common data base derived from all present-day test sites. This evaluation would suggest the optimal discrimination procedure using regional waves, and would also define areas of needed research."

In order to address the issue of regional discrimination, Taylor *et al.*, (1989) analyzed a large number of western United States earthquakes and explosions recorded at four broadband LNN seismic stations. Twelve of the most promising regional discriminants outlined in Pomeroy *et al.*, (1982) were examined. The discriminants were evaluated by closely following the descriptions given in previous studies. This included filtering the broadband data to simulate the different instruments used in the original studies and taking measurements in the same velocity windows and frequency bands. The performance of individual discriminants, and the combination of discriminants at individual stations and the four-station network were evaluated using a multivariate analysis technique. Subsequent work involved the application of artificial neural networks using attenuation-correction signal spectra to discrimination (Dowla *et al.*, 1990).

The dataset for this study consisted of 233 NTS explosions and 130 Western United States earthquakes in the magnitude range of about 2.5 to 6.5 recorded at four broadband seismic stations operated by Lawrence Livermore National Laboratory (LLNL; Figure 1). The stations surround NTS at distances of about 200 to 400 km. The propagation paths for the earthquakes range from approximately 175 to 1300 km and are confined mainly to the Basin and Range.

Most of the discriminants evaluated were based on the expected physical differences between earthquakes and explosions. For example, earthquakes result from the sudden release of stored elastic energy along a fault surface. The shearing along the rupture surface releases a large amount of shear energy relative to compressional energy. Thus, the shear phases (S, L_g, Rayleigh, and Love) are expected to be large relative to the compressional phases (P and P_g). In contrast, a pure explosion source is a center of compression and, in theory, releases only P waves and Rayleigh surface waves. A typical explosion seismogram is therefore expected to have much more compressional energy relative to the late-arriving shear energy.

Earthquakes and explosions are also expected to have different time histories associated with their energy releases; as a result, they will radiate different spectral shapes. These spectral shapes are also critically dependent on the physical properties of the near-source material and on secondary effects such as spallation of the surface layers above an explosion.

Figure 2 shows examples of seismograms and associated spectra for an earthquake and explosion of similar sizes (m_b ~ 4.2) occurring at NTS and recorded at the station ELK (~400 km). The earthquake is characterized by strong, late-arriving surface waves that are poorly developed for the explosion. This is the basis of the m_b - M_S discriminant: for an earthquake and an explosion of similar m_b, the earthquake will generally have a greater M_S. Spectral differences are also observed between the two sources. Although the low frequency spectral levels are similar, the earthquake is characterized by more high-frequency energy than the explosion.

Twelve regional discriminants from Pomeroy *et al.*, (1982) were selected that appeared to have promising discrimination potential. These can be divided into

three broad categories: long-period time-domain amplitudes, short-period time-domain amplitudes, and spectral ratios. The long-period amplitudes use the ratios of the surface-wave to body-wave amplitudes and include both measurements of Love and Rayleigh waves and of higher mode surface waves. The short-period discriminants consist of amplitude ratios of the prominent regional phases (such as L_g to P_g). The spectral ratios were generally formed by comparing the frequency content in different frequency bands for a given phase.

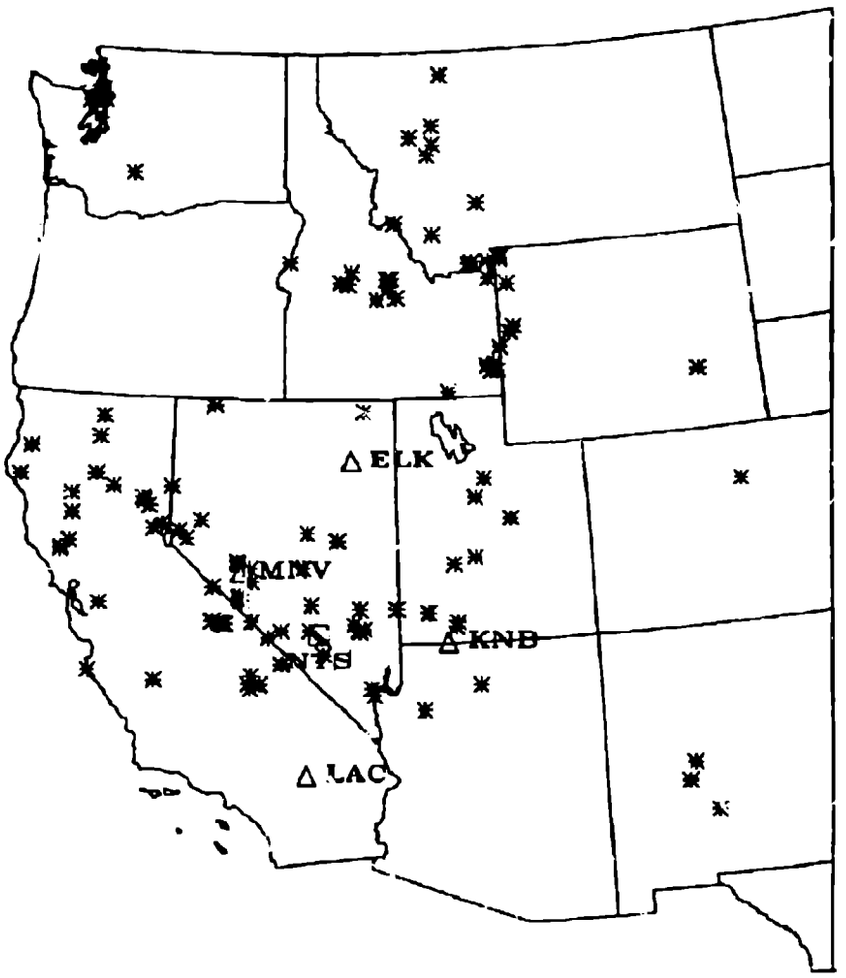

Figure 1. Map of the western United States showing earthquakes, NTS, and locations of four broadband seismic stations used in the study of Taylor *et al.*, (1989).

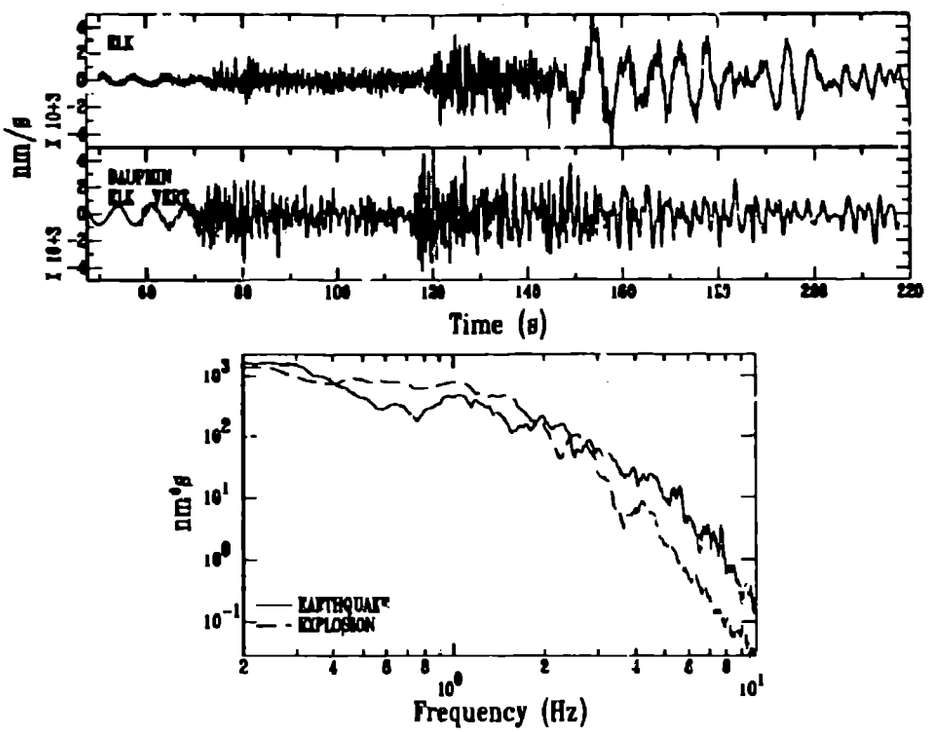

Figure 2. Examples of seismograms and spectra from an earthquake and a nuclear explosion of similar sizes (m_b ~ 4.2) both occurring on NTS and recorded at the station ELK (~400 km). Note that the large, late-arriving surface waves from the earthquake are poorly developed for the explosion (although the relative amplitudes for the other phases are similar); this is the basis of the m_b - M_S discriminant. L_g spectra from the seismograms shown in lower portion of figure. Note the existence of more high frequency energy for the earthquake relative to the explosion; this is the basis of the spectral-ratio discriminant.

The onset times of P_n, P_g and L_g were measured by an analyst and were used to define measurement windows for certain discriminants. Thus, a total of 144 measurements (based on 36 variables per station × 4 stations) was possible for each event. However, because of problems such as weak signals, recording or processing errors, and station unavailability, none of the events has a complete set of reliable measurements.

Examples of discriminants averaged for the four-station network are illustrated in Figure 3. Two of the plots in Figure 3 illustrate the performance of long-period discriminants, comparing the relative energy of Love and Rayleigh waves to body waves. As discussed above, an earthquake source is expected to generate more shear energy than an explosion source. In theory, a pure compressional source does

not generate Love waves. However, explosions can cause the release of stored elastic energy in the Earth's crust, and measurable Love waves are often observed.

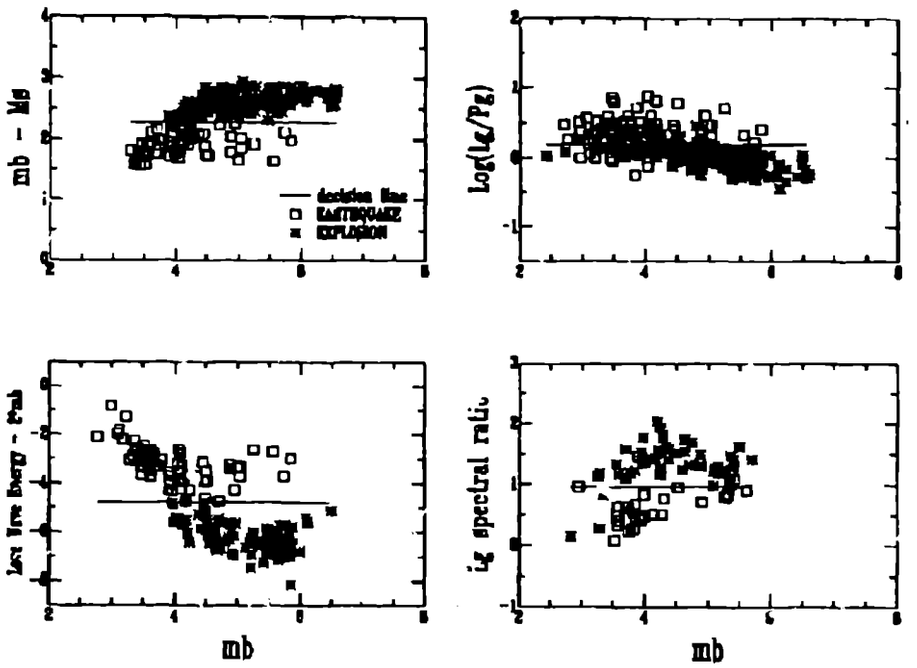

Figure 3. Discrimination plots and decision line for western U.S. earthquakes (open squares) and NTS nuclear explosions (asterisks). $m_b \cdot M_S$ is shown in upper left, Love wave energy in lower left, L_g/P_g amplitude ratio (upper right), and the 1 to 2 Hz and 6 to 8 Hz L_g spectral ratio in the lower right [see Taylor *et al.*, (1989) for details].

In general the performance of the long-period discriminants was quite good. However, small magnitude events do not efficiently generate long-period surface waves, and signal-to-noise ratios are often quite poor. For the $m_b \cdot M_S$ discriminant, it was often not possible to obtain wave measurements from explosions for frequencies < 0.1 Hz for m_b < 3.5 to 4.0. In contrast, earthquake M_S values were obtained for m_b values down to about 2.5. This difference in lower M_S thresholds for earthquakes than for explosions could conceivably be used to discriminate between the two populations at low magnitudes (using negative evidence).

The $m_b \cdot M_S$ discriminant was extended to smaller magnitudes by calculating the scalar seismic moment, M_0, (Patton and Walter, 1993; Woods *et al.*, 1993). The seismic moment is an improved method for estimating low-frequency amplitude levels and when plotted versus m_b results in improved earthquake/explosion separation for m_b < 4. However, the M_0 determination is

model dependent, and an assumption must be made regarding event type (e.g. deviatoric versus isotropic) and depth from which Green's functions can be calculated.

An example of a short-period time-domain discriminant (L_g/P_g amplitude ratio) is illustrated in Figure 3. This discriminant basically compares the short-period ratio of shear and compressional energy; earthquake sources are expected to produce a higher ratio than explosions. The data show that there is a tendency for the ratio to be higher for earthquakes than for explosions, but the scatter in the measurements is high, particularly for the earthquakes, and the results are inconsistent. The results from this discriminant are typical of many of the short-period discriminants. As will be discussed below, more recent studies by Walter *et al.*, (1994) show that the L_g/P_g discriminant performs significantly better when computed at higher frequency (6 - 8 Hz).

The short-period regional phases propagate efficiently, and the signal-to-noise ratios are generally good resulting in many measurements. However, the nature of the generation and propagation of many of these regional phases is quite complex. It has been clearly documented from both observational and theoretical studies that complex crustal structure has a dramatic effect on regional phases. The long-period surface waves have longer wavelengths (~30-80 km) than L_g and P_g and tend to smooth out the effects of velocity heterogeneity. In contrast, L_g and P_g waves have shorter wavelengths (~4-6 km) and can be dominated by scattering effects resulting in very complicated signatures.

An example of an L_g spectral ratio discriminant is shown in Figure 3. This discriminant was computed as part of a follow-on pilot study motivated by Murphy and Bennett (1982) (Taylor *et al.*, 1988) and was applied to 72 earthquakes and 64 explosions. The 1-2 to 6-8 Hz spectral ratio was computed for each of the three phases (P_n, P_g, and L_g). The spectral ratio discriminant appears to be as good as any of the discriminants tested on narrow band recording systems, particularly at low magnitudes. The apparent success of this discriminant is based on the observation that earthquakes produce more high frequency energy than the explosions for magnitudes less than ~4.5 to 5.5. As discussed above, the long-period discriminants show good separation between earthquake and explosion populations, but the measurements are difficult to make at low magnitudes. In contrast, the spectral ratio discriminant is easy to measure and involves only a simple distance correction. Our studies showed that a few of the explosions were characterized by low spectral ratios and were consistently misclassified. These explosions were found to be "overburied"(i.e., they were detonated at depths greater than necessary for containment).

Subsequent studies have shown that the spectral ratio may be affected by spallation of the surface layers above the explosion (Taylor and Randall, 1989) or by material effects close to the explosion (Taylor and Denny, 1991). Spall is defined as the parting of near-surface layers above a buried explosion. It is thought to be caused by the tensile failure that is the result of the interaction of an upgoing compressional wave with a downgoing tensile wave reflected from the free surface. The spalled surface layers are sent into ballistic free fall and eventually impact with the earth. The result is an energy increase in the 0.2-2 Hz frequency band. Thus, it was suggested that the signals from explosions detonated at normal containment depths are contaminated by spall and have a higher spectral ratio.

Subsequently, Taylor and Denny, (1991) postulated that near-source nonlinear material effects caused the difference in spectral ratios for events in different media at a given yield. Basically, explosions detonated in weak, porous rock are observed to be deficient in high-frequency energy relative to those in high-strength, saturated rocks. Thus, the spectral shape appears to be an indicator of near-source material properties and Taylor and Dowla (1991) used this fact to better constrain yield estimates of NTS explosions.

More recent work using spectral ratios between normal-depth and over-buried NTS explosions has indicated a more complicated secondary source affecting the excitation of L_g waves from explosions (Patton and Taylor, 1994). It was suggested that the secondary source is represented by a compensated linear vector dipole (CLVD), and L_g is generated by near-source scattering of R_g waves into body waves that become trapped in the crust.

The misclassification performance of individual discriminants generally ranges from a few percent to a maximum of 40% at individual stations and to 25% when network averages are used. (These misclassification percentages only apply to those events for which measurements could be obtained and generally represent 50-75% of the total available data.)

2.1 MULTIVARIATE DISCRIMINATION

To reduce misclassification probabilities, we combined certain discriminants. For example, the m_b - M_S discriminant works well for m_b > 4, and the spectral ratio discriminant is effective at low magnitudes. Standard multivariate classification techniques can be used to define a discrimination function that combines the discriminants in an optimum fashion, thereby reducing misclassification probabilities.

We investigated the utility of the multivariate discrimination technique at each of the individual stations and for the four-station network. For each event, the measured discrimination parameters can be thought of as forming a vector pointing to a location in multidimensional hyperspace. The dimension of the hyperspace is defined by the number of parameters measured for a particular event. The multivariate analysis is used to compute a discriminant function that defines a surface providing the maximum separation between the earthquake and explosion populations (Figure 4). For example, the four discriminants in Figure 3 form a four-element vector that identifies a point in a four-dimensional hyperspace.

It is necessary to transform the measurements into variables that are insensitive to magnitude, path, or features of the nuclear test program. For example, m_b is not acceptable as a discrimination parameter, but m_b - M_S is. If we had chosen only earthquakes with m_b < 4 and explosions with m_b > 4, then it would appear that any new, low magnitude event would be an earthquake. In reality, this apparent separation is an artifact of our data selection process, and it would be possible to detonate an explosion with m_b < 4 that would be misclassified on the basis of magnitude alone. However, m_b - M_S provides a measure of the body-wave to surface-wave amplitude ratio (with appropriate distance corrections) and has a fundamental physical basis for separating earthquakes and explosions.

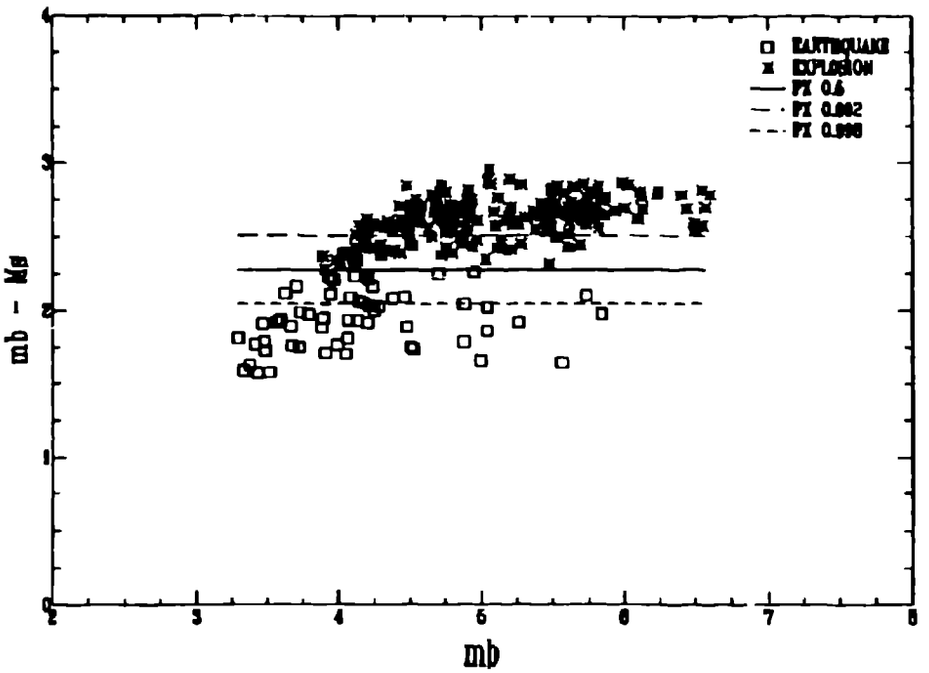

Figure 4. Examples of different decision lines based on different choices of prior probabilities of occurrence and misclassification costs applied to the m_b - M_S discriminant (see text for details).

The multivariate discrimination function takes into account (1) the *a priori* probability that a recorded event is an earthquake or an explosion and (2) the costs associated with misclassification. In monitoring a CTBT, most events recorded by an in-country network are expected to be earthquakes or industrial explosions; therefore, the *a priori* probability of observing an explosion would be set at some small number. The misclassification costs depend wholly on political judgments. This is illustrated in Figure 4 for the m_b - M_S discriminant. The decision lines PX are controlled by the product $C(Q|X)P(X)$, where $P(X)$ is the *a priori* probability that a recorded event is an explosion, and $C(Q|X)$ is the cost associated with misclassifying an explosion as an earthquake. In a CTBT context, $P(X)$ would be expected to be a low value. Thus, PX 0.998 indicates a high cost associated with misclassifying an explosion [$C(Q|X)$ large]. This results in numerous false alarms. PX 0.002 indicates a high cost associated with misclassifying an earthquake [$C(X|Q)$ large]. This results in many misidentified explosions (missed violations). PX 0.5 is the line that best separates both populations, e.g., $C(Q|X) = C(X|Q)$ and $P(X) = P(Q)$. It is common to assume equal prior probabilities and equal misclassification costs (PX 0.5), which result in minimizing the average estimated misclassification probabilities.

Applying the multivariate technique to individual stations for the entire data set shows misclassification rates ranging from 3-10% for explosions and 4-26% for earthquakes. Multistation discrimination shows misclassification probabilities of 0-2% for explosions and of 3-4% for earthquakes.

A breakdown of the misclassification probabilities as a function of m_b is shown in Figure 5 for the individual stations and the network. These plots show that

- Misclassification rates are generally higher for $m_b < 4$
- Higher misclassification rates are observed for earthquakes than for explosions.
- Significant differences in discrimination capability are observed between the four stations

The higher misclassification rates for the low magnitude events may be due to poorer signal-to-noise ratios, particularly for the long-period measurements, which appeared to perform so well (Figure 3). Part of this problem may be that, in general, low magnitude events had fewer usable measurements on which to base a classification. The higher misclassification rates for earthquakes are probably due to their having a wider variety of propagation paths, distances, depths, and source mechanisms. Because all of the explosions were from the same region, it was difficult to separate out complications that can be attributed to the source or to propagation. If these explosions had been more widely distributed over the western U.S., more variability in the explosion data set might have been observed and discrimination performance might have been degraded.

2.2 HIGH-FREQUENCY DISCRIMINATION

The above described work has recently been extended by Walter *et al.*, (1994) to include higher frequency *P*-wave to *S*-wave phase ratios and L_g - coda spectral ratios. The dataset consisted of 130 NTS nuclear explosions, a 1 kiloton chemical explosion (the Non-Proliferation Experiment, NPE; Denny and Zucca, 1993) and 50 earthquakes. Importantly, most of the earthquakes occurred as two sequences on the NTS so that path effects could be minimized. For both sequences, aftershock surveys were conducted so good information was available regarding locations, depths, and focal mechanisms. The magnitude 5.7 Little Skull Mountain earthquake occurred in June 1992 and was followed by numerous aftershocks occurring between 6 and 12 km depth (Walter, 1993). The data analysis concentrated on the LNN stations MNV and KNB since the Landers, California earthquake (that occurred the day before the Little Skull Mountain earthquake) knocked out the LAC station and ELK was operating only intermittently during the summer of 1992. In the spring of 1993 and 1994 a series of earthquakes having magnitude less than 3.8 occurred in Rock Valley approximately 10-20 km southeast of the Little Skull Mountain sequence at unusually shallow depths.

Examples of high frequency (6-8 Hz) P_n/L_g and P_g/L_g spectral ratios and L_g-coda spectral ratio [(1-2)/(6-8) Hz] are shown in Figure 6. Other frequency bands were examined and although using wider spaced frequency bands appeared to provide better separation, signal to noise limitations restricted the number of events. The L_g-coda spectral ratio appeared to have slightly improved performance over the direct L_g spectral ratio because of reduced interstation variability (Mayeda, 1993).

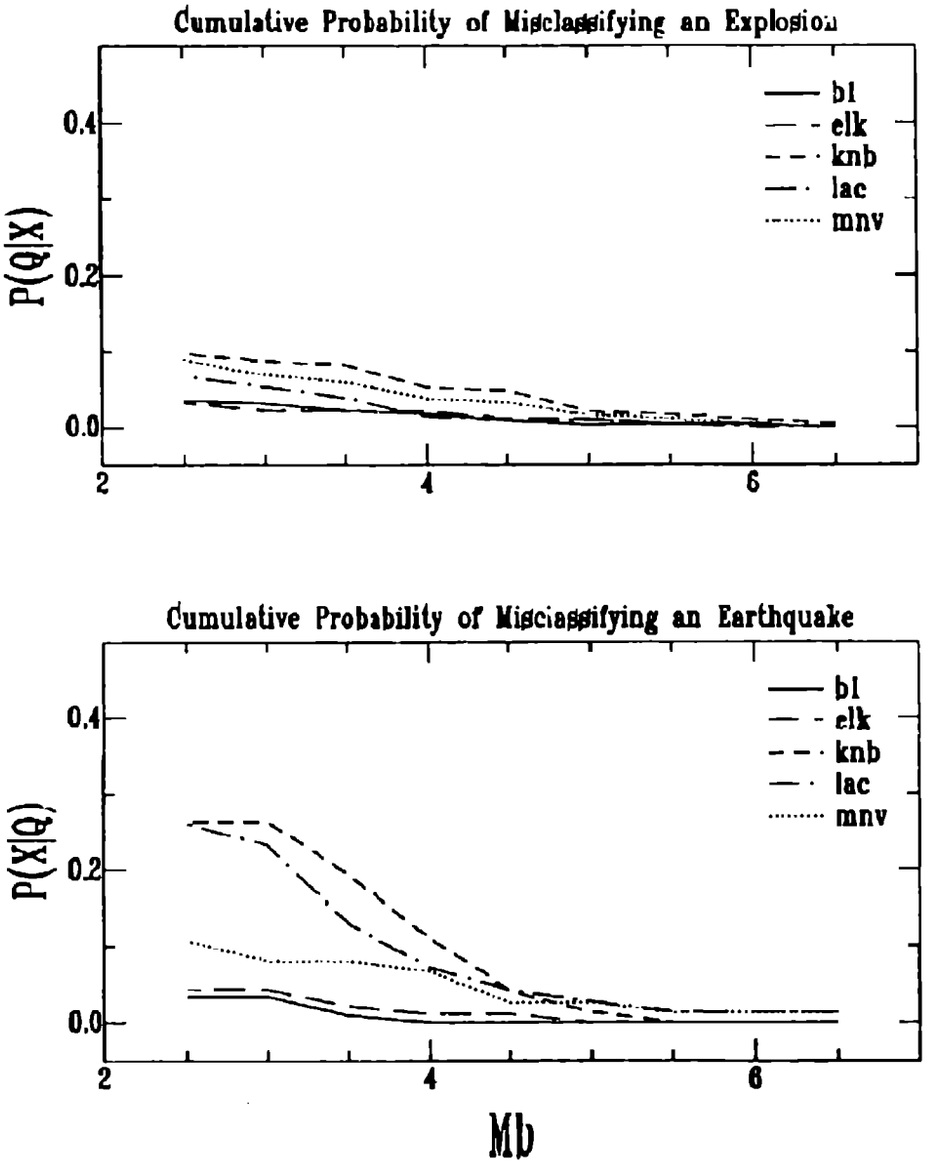

Figure 5. Probabilities for misclassifying an explosion as an earthquake - a missed violation (top) and an earthquake as an explosion - a false alarm (bottom) from multivariate analysis of western U.S. earthquakes and NTS explosions.

A number of interesting features can be observed on the discrimination plots in Figure 6. Both the P_n/L_g and P_g/L_g ratios show no strong magnitude dependence.

Significant differences in station performance were observed between KNB and MNV. Shallow events showed higher ratios at KNB for both P/L_g discriminants. In general, the P_n/L_g worked better at MNV and the P_g/L_g worked better at KNB. Walter *et al.*, (1994) divided the explosion population into two groups based on a combination of gas-filled porosity (GP) and strength (estimated by the product $\rho\alpha^2$). The P_g/L_g ratio appears to show a strong dependence on near-source material properties with the low GP - high strength materials having larger ratios (better separation from earthquakes). Additionally, for the P_n/L_g ratio, the shallow earthquakes have higher ratios (mainly due to high values at KNB) and plot with the explosions. No such effect is observed for P_g/L_g.

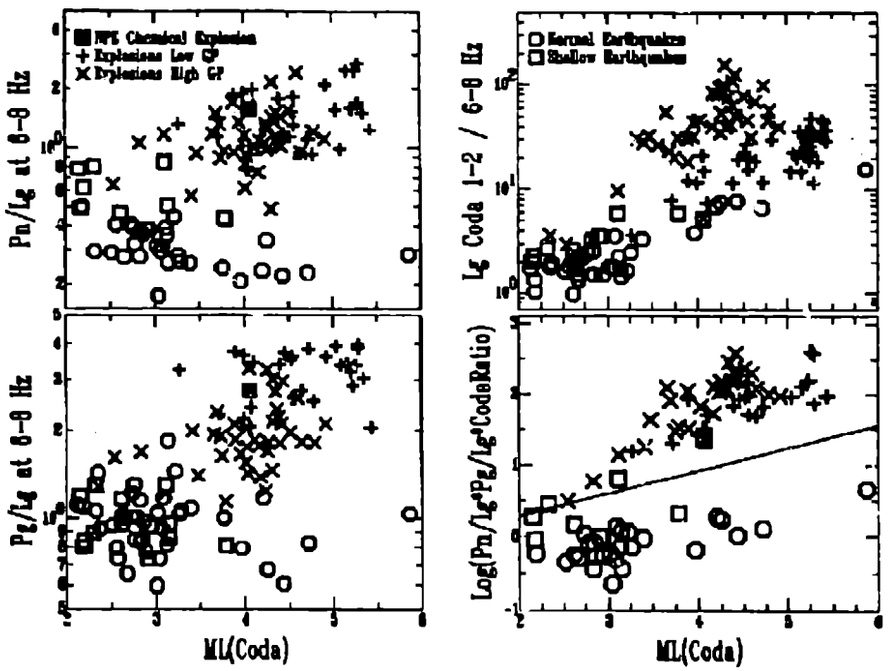

Figure 6. Examples of MNV-KNB averaged discriminants for NTS explosions and earthquakes from Walter *et al.*, (1994). Explosions separated on basis of strength and gas-filled porosity (GP) and Non Proliferation Experiment (NPE). P_n/L_g (upper left); P_g/L_g (lower left); L_g-coda spectral ratio (upper right); combined (lower right).

The 1-2/6-8 Hz spectral ratios for the L_g coda is shown in the upper right hand corner of Figure 6 and the observed patterns are similar to those observed by Taylor *et al.*, (1988). A strong magnitude dependence is observed that is presumably due to corner frequency scaling (Taylor and Denny, 1991). Additionally, the high gas porosity - low strength materials have the highest L_g spectral ratios and show better separation from the earthquakes.

Because of the different dependencies of the discriminants on material properties they could be effectively combined to reduce the number of misclassifications. Figure 6 shows the combined P_n/L_g , P_g/L_g , and L_g coda spectral ratio where excellent discrimination is observed between the explosions and the normal depth earthquakes. The only two misclassified events were two of the shallow Rock Valley earthquakes resulting in a false alarm rate of 6% (earthquakes classified as explosions) and no missed violations (explosions classified as earthquakes).

3. Analysis of Misclassified Events

In monitoring a CTBT, particular attention must be paid to events that are misclassified. Misclassified events fall into two groups: 1) missed violations (e.g. nuclear explosions that look like earthquakes) and 2) false alarms (e.g. naturally occurring events that look like nuclear explosions). Both have important implications for nuclear test ban monitoring. Obviously, missed violations imply that some nation is not concurring with the nuclear test ban treaty and is undertaking a clandestine test program. False alarms are an important issue because they can result in a raising of regional tensions between neighboring proliferant nations. It is important that the CTBT monitoring network is able to detect clandestine nuclear explosions (or at least act as a major deterrent to a nation wishing to evade the treaty) and to resolve false alarms. Both types of events will require special event studies. In the following, we show examples of two special event studies (a missed violation and a false alarm) using events from the study of Taylor *et al.*, (1989).

Understanding why anomalous events are anomalous is important because we can use this information to identify opportunities for evasion. The most important question is:

Was an event misclassified because of some factor that can be controlled by the country conducting the test?

If the answer is yes, this factor provides an opportunity for evasion. A classic example of such a factor is cavity decoupling during which the amplitudes of seismic waves from an explosion detonated in a large cavity (such as a salt dome) can be reduced by a factor of ~70. Detailed analysis of anomalous events identified in our study has led to an improved understanding of explosion source physics and the generation of seismic waves. It is important to focus analysis on low magnitude events (m_b < 4), which pose the most difficulties.

3.1 MISSED VIOLATION

The study (Taylor *et al.*, 1988) of spectral discriminants showed good separation down to at least m_b = 3.5. However, a few explosions conspicuously plotted lower in the earthquake population (Figure 3). Two of these three explosions were overburied (i.e., they were detonated at depths greater than necessary for containment) and were characterized by a higher frequency content than normally buried explosions.

One explosion, QUESO, was not significantly overburied but showed a low spectral ratio. We noticed that a large (~564 m^3) funnel-shaped region filled with unconsolidated sand existed directly above the QUESO detonation point (Figure 7). To determine if this region could have affected the seismic signals, we compared the QUESO signals with those from a nearby explosion, PERA, of similar size and burial depth (Taylor and Rambo, 1989). Comparison of the spectra from accelerometer records taken 90 m from the explosions show remarkable similarities to those at 400 km (Figure 8). This indicates that the spectral characteristics from explosion sources are established at very close ranges.

Our modeling suggests that the anomalous region above QUESO may have partially decoupled the upgoing energy resulting in a reduction of low frequency spectral levels. Additionally, the unconsolidated sand and voids above QUESO strongly attenuated the outgoing shock wave, therefore reducing the energy available for pore collapse and the fracturing of surrounding rock. This, in turn, resulted in the radiation of more impulsive, shorter-duration waveforms that produced a less-rapid high frequency spectral decay. These two effects resulted in a lower spectral ratio for QUESO.

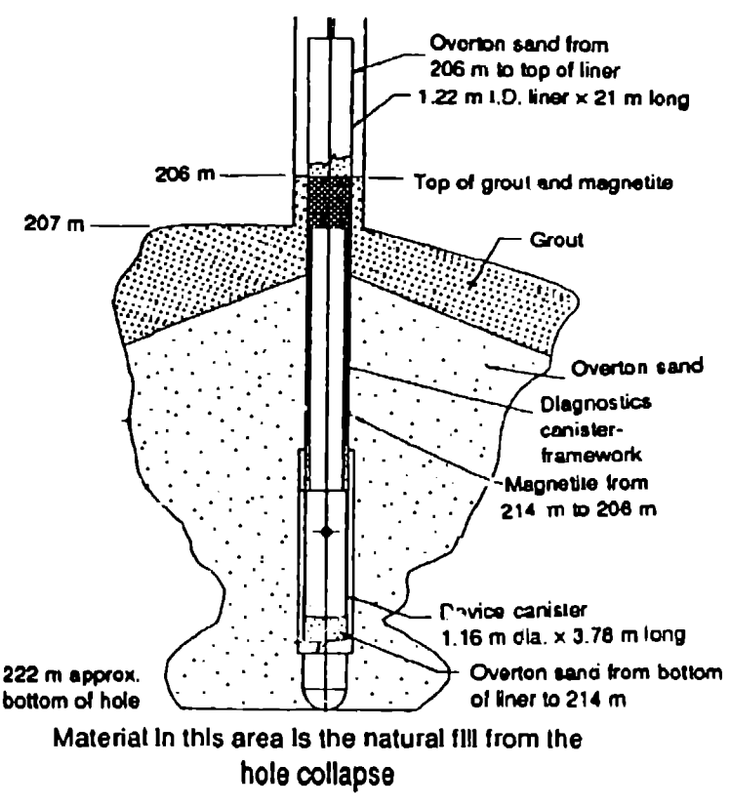

Figure 7. QUESO emplacement configuration.

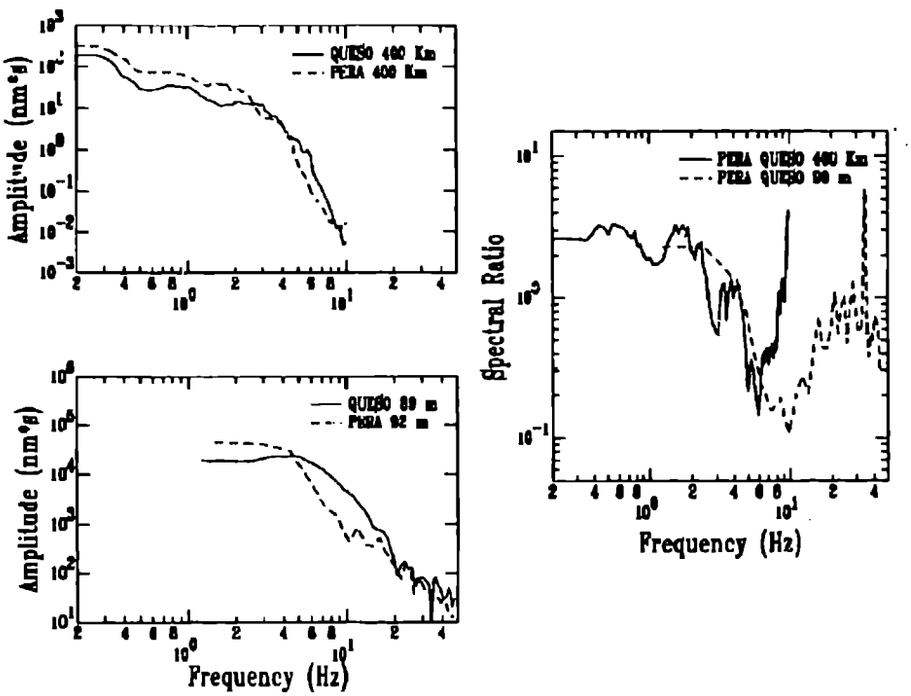

Figure 8. L_g displacement spectra at LLNL station ELK (distance ~ 400 km) for PERA and QUESO (upper left) compared with close-in displacement spectra (lower left) from emplacement hole gages (~90 m). PERA/QUESO spectral ratios at ELK and emplacement hole gages are compared at the right. Close similarity of the two spectral ratios suggests that spectral characteristics are established very close to the source.

3.2 FALSE ALARM

For CTBT research, much attention is paid to the study of chemical mining explosions. The large number of mining explosions can cause problems for any monitoring system. Much of the concern over mining regions is that they can provide the cover for hiding a decoupled nuclear explosion. Mining operations are often characterized by high seismicity rates and can provide the cover for excavating voids for decoupling. Chemical explosions (seemingly as part of normal mining activities) can be used to complicate the signals from a simultaneous decoupled nuclear explosion. Numerical simulations suggest that it may be possible to mask a 0.05 kt fully tamped (or 1.5 to 5.0 kt fully decoupled) nuclear explosion in a 1 kt ripple-fired quarry blast (Barker and McLaughlin, 1992). Similarly, Smith (1992) found that a single explosion (fully tamped) could be detected if its size exceeds about 10% the size of a simultaneous ripple-fire explosion. This suggests that it may be possible to mask a 0.5 kt decoupled nuclear

explosion in a 50 ton mine blast (assuming a factor of 100 decoupling). Thus, most concern about mines has dealt wi h the issue of missed violations to a test ban treaty.

In the study of Taylor (1994), the problem of false alarms associated with mining activities was raised. False alarms are an important issue because they can result in a raising of regional tensions between neighboring proliferant nations. An example of a false alarm was the April 28, 1991 event located near the Pakistan-Indian border. The Pakistanis originally thought it was located near the Indian test site and its location was ultimately resolved through the use of additional seismic data from open stations (Turnbull, 1993).

As part of the discrimination study of Taylor *et al.* (1989), one earthquake was consistently classified as an explosion. The magnitude 3.5 disturbance occurred on May 14, 1981 (MAY1481) and was conspicuous in its lack of Love waves, relative lack of high-frequency energy, low L_g/P_g ratio, and high m_b - M_S. Additionally, a moment-tensor solution by Patton and Zandt (1991) indicated the event had a large *implosional* component. The event occurred in the Gentry Mountain coal mining region in the eastern Wasatch Plateau, in central Utah (Figure 1). Previous microearthquake studies in the region have demonstrated the existence of numerous small implosional events associated with the mining activities. For comparison, a nearby "normal" tectonic earthquake of M_L 4.2 that occurred on May 24, 1980 (MAY2480) 93 km to the northwest of MAY1481 was analyzed. The MAY2480 event was also processed as part of the discrimination study and correctly classified as an earthquake.

Figure 9 compares KNB seismograms from the MAY2480 and MAY1481 events with the NTS ATRISCO collapse and the NTS nuclear explosion PERA. All of the events are of similar magnitude and distance range from KNB and show some interesting similarities and differences. First, the MAY2480 event shows a much higher frequency content, better developed Lg and Rayleigh waves, and shorter coda than MAY1481. The MAY1481 event is characterized by a narrow band, long reverberating wave train with few well-defined phases except P_n and P_g. Interestingly, the MAY1481 event is more comparable in appearance to the ATRISCO collapse than the earthquake or the nuclear explosion.

Contact was made with the mining engineers at U.S. Fuel Company who operate the Gentry Mountain mine. Although they do not keep records, they did vividly remember a major collapse that occurred on May 14, 1981. They had restarted mining in some old workings and were having a very difficult time with collapses and estimated that the room size that collapsed could have been as large as 150 m on a side. Using the thickness of the coal seam and the size of the room, Taylor (1994) estimated that the collapse could have caused an event of the size of that observed for MAY1481.

Using group velocity dispersion from the MAY2480 event, a velocity model was derived from the source region to the KNB station that gave reasonable appearing synthetic seismograms given the double-couple source mechanism and depth of Patton and Zandt (1991). An equivalent elastic point-source representation was used to model the MAY1481 event as a tabular excavation collapse. The model consisted of two terms: a vertical force representing the detachment, free fall, and impact of the ceiling material, and a vertical moment related to the mass transfer from ceiling to floor (schematically illustrated in Figure

10). The time function convolved with the vertical point-force response is a modification of the spall time function of Day *et al.*, (1983) and Stump (1985). The collapse time function is also illustrated in Figure 10.

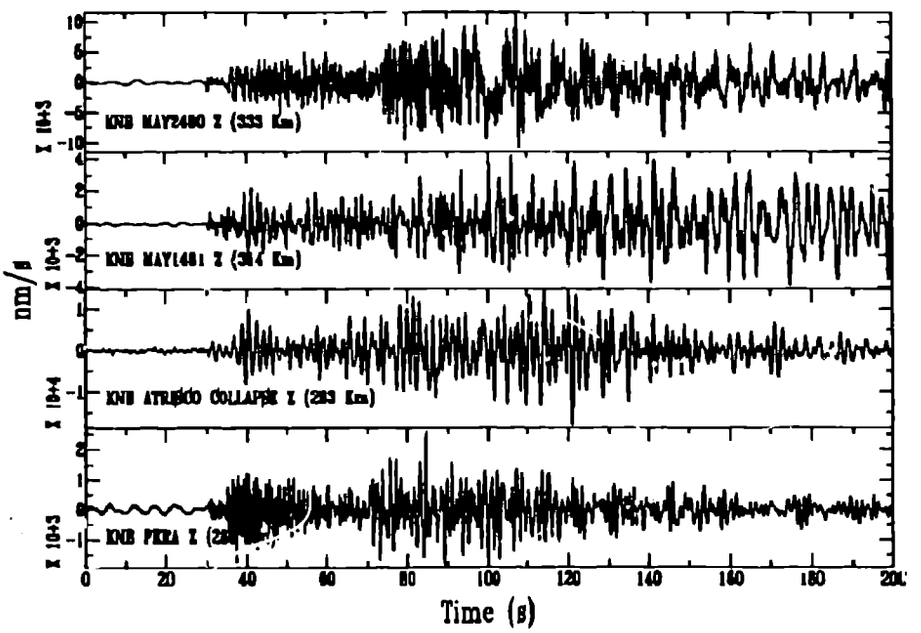

Figure 9. Comparison of broadband seismograms at station KNB for four different events. From the top; MAY2480, MAY1481, ATRISCO collapse (from NTS), and NTS nuclear explosion PEKA. The epicentral distance for each event to KNB is labeled in parentheses.

The first portion of the time function represents the detachment of the ceiling and rebound of the region around the excavation during free fall of the ceiling material. The second portion represents the subsequent impact. The model is constructed such that momentum is conserved. The time between the initiation and impact is derived from simple ballistics and the whole function is smoothed to represent finite time duration (as suggested by Stump, 1985).

Simple energy considerations based on the magnitude for the MAY1481 event suggest that collapsed mass was approximately $2.8 \times 10^8 Kg$ for a 4 m coal seam. Once the vertical point-force and vertical dipole Green's functions are computed forward modeling was used to obtain a direct estimate of the collapsed mass. Since the coal seam was 4 m thick, the time between initiation of collapse and impact was set to be 1 second and a smoothing operator of 0.4 second was used. The mass was adjusted until a reasonable match was obtained for the Rayleigh waves. A mass of $7.0 \times 10^8 Kg$ provided a reasonable match in amplitude and observed and calculated waveforms are shown in Figure 11. For the broadband seismograms, the overall characteristics are also matched quite well including the

amplitudes. The long reverberating wave train is presumably due to the shallow depth of the source (200 m) and the resultant energy being trapped in the low-velocity near-surface layers. Thus, the collapse model generates seismograms that appear to match the data at KNB quite well.

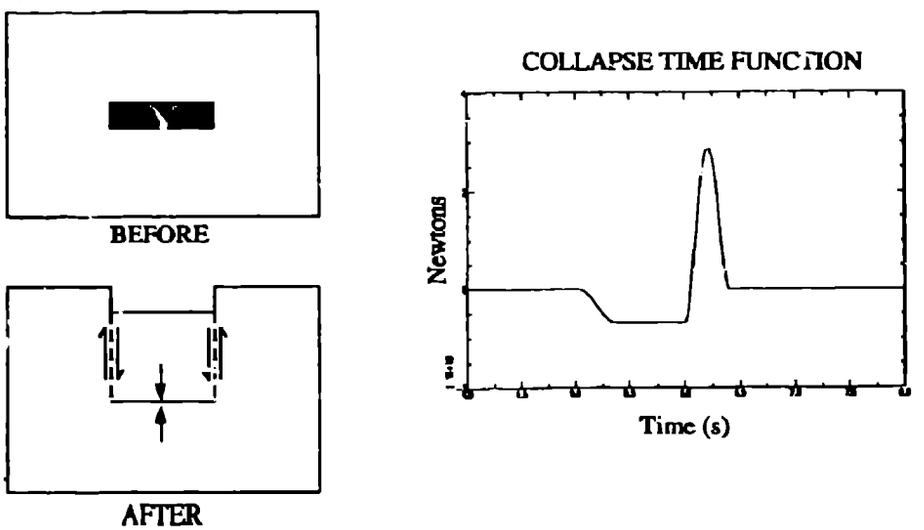

Figure 10. Schematic showing the model used to simulate the tabular excavation collapse. The figure on the upper left shows the room prior to collapse. The lower left figure shows the collapse and the various dipoles and shear couples. It is assumed that the shear couples cancel. The right figure shows the collapse time function used in the modeling (see text for details).

The modeling performed above is very simple and non unique. If the discrimination database and the abundant information about the Gentry Mountain mining activities were not available, the MAY1481 event would probably remain unresolved. Thus, this study pointed out the importance of having high-quality broadband seismic data, discrimination calibration data, and information on mining activities from regions being monitored.

4.0 Conclusions

We have reviewed a number of discrimination studies performed in the western U.S. using broad band regional seismic data. These studies are important because they represent the only large discrimination studies involving a large number of nuclear explosions and earthquakes in a single geophysical region. Additionally, excellent ground truth information is available for the NTS explosions that allow for the determination of the physical basis of the regional discriminants. This information is critical for evaluating the potential of various regional discriminants in new regions to be monitored under a CTBT from which no explosion information

is available. The CTBT monitoring network will have to have a high probability of identifying clandestine nuclear explosions while minimizing the number of false alarms. Resolution of false alarms will be an important aspect of CTBT monitoring and will involve special event studies. As shown from two examples of special event studies, it will be necessary to have high-quality, broad band seismic data, and a significant database of ground truth information (e.g. seismic data from known events and information regarding the source of anomalous seismicity). The collection of this information will be an ongoing process once the CTBT monitoring network is established.

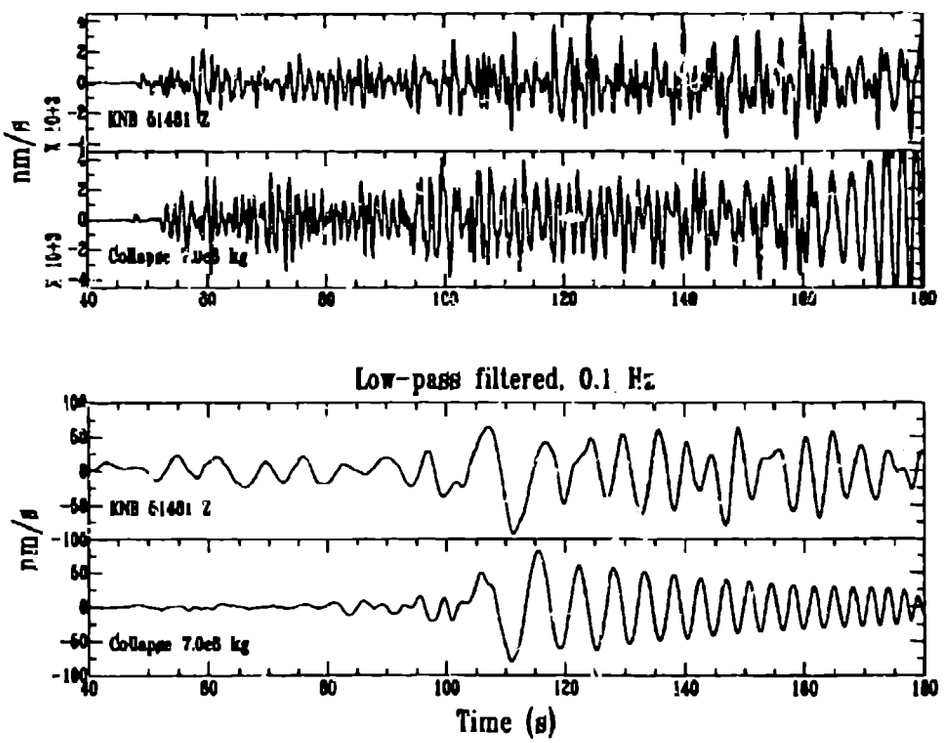

Figure 11. Comparison of calculated and observed seismograms at station KNB for the MAY1481 event using the collapse model described in the text and shown in Figure 10. Top two traces and bottom two traces are low-pass filtered at 5 Hz and 0.1 Hz, respectively.

Acknowledgments

The author wishes to thank Bill Walter for supplying preprints and figures of his work. Brian Stump reviewed the manuscript even though he is a busy guy. Thanks also to Lanny Piotrowski for preparing the camera-ready manuscript under short notice. This work is performed under the auspices of the U.S. Department of Energy by Los Alamos National Laboratory under contract W-7405-ENG-36 and by the Lawrence Livermore National Laboratory under contract W-7405-ENG-48.

References

1. Barker, T.G. and K.L. McLaughlin (1992). Numerical models of quarry blast sources, in Proceedings of the 14th Annual PL/DARPA Seismic Research Symposium, 15-21.

2. Baumgart, D.R. and G.B. Young (1990). Regional seismic waveform discriminants and case-based event identification using regional arrays, *Bull. Seism. Soc. Am.*, **80**, 1874-1892.

3. Day, S.M., N. Rimer, and J.T. Cherry (1983). Surface waves from underground explosions with spall: Analysis of elastic and nonlinear source models, *Bull. Seism. Soc. Am.*, **73**, 247-264.

4. Denny, M.D. and J.J. Zucca (1993). DOE non-proliferation experiment includes seismic data, *Trans. Am. Geophys Un.*, **74**, 527.

5. Dowla, F.U., S. R. Taylor, and R.W. Anderson (1990). Seismic discrimination with Artificial Neural Networks: Preliminary results with regional spectral data, *Bull. Seism. Soc. Am.*, **80**, 1346-1373.

6. Fisk, M.D., H.L. Gray, and G.D. McCartor (1993). Applications of generalized likelihood ratio tests to seismic event identification, PL-TR-93-2221, Phillips Laboratrory, Hanscom AFB, MA.

7. Hannon, W.J. (1985). Seismic verification of a comprehensive test ban, *Science*, **227**, 251-257.

8. Mayeda, K.M. (1993). $m_b(L_g$ Coda): A stable single station estimator of magnitude, *Bull. Seism. Soc. Am.*, **83**, 851-861.

9. Murphy, J.R. and J.J Bennett (1982). A discrimination analysis of short-period regional seismic data recorded at Tonto Forest Observatory, *Bull. Seism. Soc. Am.*, 72, 1351-1366.

10. Office of Technology Assessment (1988). Seismic verification of nuclear testing treaties, OTA-ISC-361, *U.S. Government Printing Office*, Washington, D.C.

11. Patton, H.J. and S.R. Taylor (1993). Analysis of L_g spectral ratios from NTS explosions: Implications for the source mechanisms of spall and the generation of L_g waves, *Los Alamos National Laboratory, Los Alamos, NM*, LAUR-93-4151, (submitted to *Bull. Seism. Soc. Am.*) , 26pp.

12. Patton, H.J. and W.R. Walter (1993). Regional moment:magnitude relations for earthquakes and explosions, *Geophys. Res. Lett.*, **20**, 277-280.

13. Patton, H.J. and G. Zandt (1991). Seismic moment tensors of western U.S. earthquakes and implications for the tectonic stress field, *J. Geophys. Res.*, **96**, 18, 245-259.

14. Pomeroy, P.W., W.J. Best, and T.V. McEvilly (1982). Test ban treaty verification with regional data-a review, *Bull. Seism. Soc. Am.*, 72, S89-S129.

15. Smith, A.T. (1989). High-frequency seismic observations and models of chemical explosions: implications for the discrimination of ripple-fired mining blasts, *Bull. Seism. Soc. Am.*, 79, 1089-1110.

16. Stump, B.W. (1985). Constraints on explosive sources with spall from near-source waveforms, *Bull. Seism. Soc. Am.*, 75, 361-377.

17. Taylor, S.R., N.W. Sherman, and M.D. Denny (1988). Spectral discrimination between NTS explosions and western U. S. earthquakes at regional distances, *Bull. Seism. Soc. Am.*, 78, 1563-1579.

18. Taylor S.R., M.D. Denny, E.S. Vergino, and R.E. Glaser (1989). Regional discrimination between NTS explosions and western U.S. earthquakes, *Bull. Seism. Soc. Am.*, 79, 1142-1176.

19. Taylor, S.R. and M.D. Denny (1991). An anlysis of spectral differences between Nevada Test Site and Shagan River nuclear explosions, *J. Geophys. Res.*, 96, 6237-6245.

20. Taylor, S.R. and G.E. Randall (1989). The effects of spall on regional seismograms, *Geophys. Res. Lett.*, 16, 211-214.

21. Taylor, S.R. and F.U. Dowla (1991). Spectral yield estimation of NTS explosions, *Bull. Seism. Soc. Am.*, 81, 1292-1308.

22. Taylor, S.R. (1994). False alarms and mine seismicity: An example from the Gentry Mountain mining region, Utah, *Bull. Seism. Soc. Am.*, 84, 350-358.

23. Turnbull, L. (1993). Goals for monitoring a nuclear explosions in a Proliferation and Comprehensive Test Ban environment, in DOE/LLNL Verification Symposium on Technologies for Monitoring Nuclear Tests Related to Weapons Proliferation, K.K. Nakanishi (ed.), *Lawrence Livermore National Laboratory, Livermore, CA*, CONF-9205166, 3-8.

24. Walter, W.R. (1993). Source parameters of the June 29, 1992 Little Skull Mountain earthquake from complete regional waveforms at a single station, *Geophys. Res. Lett.*, 20, 403-406.

25. Walter, W.R., K.M. Mayeda, and H.J. Patton (1994). Phase and spectral ratio discrimination between NTS earthquakes and explosions Part 1: Empirical observations, *Lawrence Livermore National Laboratory*, UCRL-JC-118551 Part 1, 32pp.

26. Woods, B.B., S. Kedar, and D.V. Helmberger (1993). $M_L : M_0$ as a regional seismic discriminant, *Bull. Seism. Soc. Am.*, 83, 1167-1183.